Posture similarity index: A method to compare hand postures in synergy space

Nayan Bhatt [1] , **Varadhan SKM** Corresp. [1]

[1] Department of Applied Mechanics, Indian Institute of Technology Madras, Chennai, India

Corresponding Author: Varadhan SKM
Email address: skm@iitm.ac.in

Background

The Human hand can perform a range of manipulation tasks, from holding a pen to holding a hammer. Central Nervous System (CNS) uses different strategies in different manipulation tasks based on task requirements. Several attempts to compare postures of the hand have been made. Some of these have been developed for use in Robotics and animation industries. In this study, we develop an index to quantify the similarity between two human hand postures, the posture similarity index.

Methods

Twelve right-handed volunteers performed 70 postures and lifted and held 30 objects (total of 100 different postures, each performed 5 times). Kinematics of individual finger phalanges (segments) were captured by using a 16-sensor electromagnetic tracking sensor system. The hand was modelled as a 21-DoF system and the corresponding joint angles were computed. We used principal component analysis to extract kinematic synergies from this 21-DoF data. We developed a posture similarity index (PSI), that represents similarity between posture in the synergy (Principal component) space. First, performance of this index was tested using a synthetic dataset. After confirming that it performs well with synthetic dataset, we used it to analyse experimental data. Further, we used PSI to identify postures that are representative in the sense that they have a greater overlap (in synergy space) with a large number of postures.

Results

Using synthetic data and real experimental data, it was found that PSI was a relatively accurate index of similarity in synergy space. Also, it was found that more special postures than common postures were found among “representative” postures.

Conclusion

An index for comparing posture similarity in synergy space has been developed and its use has been demonstrated using synthetic dataset and experimental dataset. In addition, we found that special postures are actually special in the sense that there are more of them in the “representative” postures as identified by our posture similarity index.

Posture similarity index: A method to compare hand postures in synergy space

Nayan S Bhatt[1], Varadhan SKM[1]

[1] Department of Applied Mechanics, Indian Institute of Technology Madras, Chennai, Tamil Nadu, India

Corresponding Author:

Varadhan SKM [1]

Department of Applied Mechanics, Indian Institute of Technology Madras, Chennai, Tamil Nadu, India

Email address: skm@iitm.ac.in

Abstract

Background

The Human hand can perform a range of manipulation tasks, from holding a pen to holding a hammer. Central Nervous System (CNS) uses different strategies in different manipulation tasks based on task requirements. Several attempts to compare postures of the hand have been made. Some of these have been developed for use in Robotics and animation industries. In this study, we develop an index to quantify the similarity between two human hand postures, the posture similarity index.

Methods

Twelve right-handed volunteers performed 70 postures and lifted and held 30 objects (total of 100 different postures, each performed 5 times). Kinematics of individual finger phalanges (segments) were captured by using a 16-sensor electromagnetic tracking sensor system. The hand was modelled as a 21-DoF system and the corresponding joint angles were computed. We used principal component analysis to extract kinematic synergies from this 21-DoF data. We developed a posture similarity index (PSI), that represents similarity between posture in the synergy (Principal component) space. First, performance of this index was tested using a synthetic dataset. After confirming that it performs well with synthetic dataset, we used it to analyse experimental data. Further, we used PSI to identify postures that are representative in the sense that they have a greater overlap (in synergy space) with a large number of postures.

Results

Using synthetic data and real experimental data, it was found that PSI was a relatively accurate index of similarity in synergy space. Also, it was found that more special postures than common postures were found among “representative” postures.

Conclusion

An index for comparing posture similarity in synergy space has been developed and its use has been demonstrated using synthetic dataset and experimental dataset. In addition,

we found that special postures are actually special in the sense that there are more of them in the "representative" postures as identified by our posture similarity index.

Introduction

Modeling hand and finger postures accurately has been of interest in Robotics and animation industry. In the animation industry, differentiation of one hand posture from another is crucial for perception of a gesture and to bring in a more "lifelike" appearance (Hoyet et al 2012). In robotics, comparison of a robotic posture with the biological (human) hand posture is useful to assess the performance of a robot (Feix et al 2013).

Studies in perception of animations have exploited the relatively lower number of dimensions that are required to distinguish between perceived postures (Hoyet et al 2012). So they have used a relatively smaller number of markers to produce postures that are perceived as different. Work in robotics has focused on development of methods to compare a robotic posture with hand posture, the "anthropomorphism index" (Feix et al 2013, Romero et al 2010). Other works have focused on exploring the low-dimensional subspace used by human hand postures (Ciocarlie & Allen, 2009, Wheatland et al 2013). This has been attempted probably because of the notion that designing better grasping robots must essentially involve learning from human grasping. These approaches attempt to compare human hand postures with those generated by a computer (animations) or by a robot (robotics). Comparison of a human hand posture with another human hand posture has not been attempted by these studies.

In the field of motor control, several studies have attempted to characterize and/or model hand postures (Santello 1998; Gentner & Classen, 2006; Cavallo et al., 2016; Leo et al 2016). Many of these studies have used Principal component analysis (PCA) to identify the dominant dimensions in the multi-dimensional space of a set of hand and finger postures (where each posture is quantified as a set of joint angles). The proportion of variance explained by these dominant dimensions have been quantified and presented in many of these studies.

However, these studies have not attempted to compare postures per se. As such, assessment of similarity is a challenging problem and some relatively sophisticated algorithms have been proposed (cf., Roweis & Saul, 2000). We believe that a method to specifically compare human

hand postures in synergy space useful in the fields of motor control, animation and robotics. We attempt to develop such a method in this paper.

In this study, we propose, define and develop an index, (posture similarity index, PSI), that quantifies similarity in the principal component ("synergy") space. We first test this index on a synthetic dataset and then with a small experimental dataset. We then use this index to study similarity across a large number of postures (100 postures, including both everyday life and special postures). Based on PSI, we identify representative postures that may reflect dimensionality of hand action in the synergy space. These representative postures are those that have a relatively large overlap in synergy space with a several postures. Further, we compare the number of everyday life postures and special postures that are found among this set of "representative postures".

Materials & Methods

Participants

Twelve right-handed volunteers (six males and six females, mean ± SD Age: 25.5 ± 1.55 years, height: 172.8 ± 5.16 cm) provided written informed consent and participated in the study. No participant had history of any neurological disorder or any trauma to upper extremity. Our experimental procedures were approved by Institutional Ethics Committee of IIT Madras (Approval number: IEC/2016/02/VSK-1/11). All participants were naïve to the purpose of the study.

Experimental Apparatus

The experimental procedure involves performing simple motor acts including specific hand postures and object manipulation. For collection of kinematic information, electromagnetic tracking sensors (Diameter 1.8mm, Resolution 1.27 microns, Static position accuracy 0.76mm, Static angular orientation accuracy 0.15 degree, Polhemus Inc., USA, Model: Liberty micro sensors) were used. For preventing interference, metallic objects were minimized in the experimental room during the experiment. Sensor placement on the dorsal side of digits (I: Index; M: Middle; R: Ring; L: Little) using double sided adhesive tape as shown in Figure 1 (A). It captures the movement of distal segment/phalanx, middle segment/phalanx, proximal segment/phalanx, and metacarpals. Distal interphalangeal (DIP), proximal interphalangeal (PIP) and metacarpophalangeal (MCPs) joint angles for I, M, R and L were derived from these

quantities; for the thumb it measures movements of distal, proximal and metacarpal segments and interphalangeal (IP), metacarpophalangeal (MCP) and carpometacarpal (CMC) joint angles were computed. The reference sensor was mounted near proximal part of the wrist between 2nd and 3rd metacarpal bone. Customized user interface was designed in LabVIEW (National Instruments) environment to collect data at 120 Hz, and offline analysis was performed using MATLAB (MathWorks, USA).

(Figure 1)

Kinematic data acquisition

The experimental setup is shown in Figure 2. Placement of sensors in lab coordinate system was designed according to biomechanical standards (Wu et al., 2005). A base posture is defined for starting of every trial. In this base posture, the hand is in pronation position with all the fingers (including the thumb) fully extended and adducted. Subjects were seated in a height adjustable chair comfortably with his/her arm resting on the table at approximately wrist level with palm facing surface of the table. A 24-inch LED monitor was placed approximately 1 meter away from the participants.

(Figure 2)

The experiment consisted of two different tasks, the first task was performing internally constrained postures which include 70 postures, and the rest 30 are constrained postures which involve object manipulation. For internally constrained postures, pictures of target postures (i.e. American Sign Language (ASL), Indian dance form Bharatanatyam) were shown to the subjects on a computer screen. At the beginning of each trial, the subject started from the base posture and reached target posture. Each trial was five seconds long. Each posture was repeated five times. Hence, subjects performed a total of 500 (100 postures x 5 trials per posture) trials. Ten seconds of rest was given to the subjects between trials to avoid fatigue. Additional rest was provided whenever subject requested during the experiment.

For the externally constrained postures, before each trial, an object was placed on predefined marked position, nearly 15 centimetres away from the hand. Subjects were then asked to lift and hold the object approximately 10 centimetres above the surface. Static posture at the end of the trial was visually compared with target posture. All the trials were carefully observed by the

experimenter and any trial in which the posture was not faithfully performed was repeated. All the postures are shown in Supplementary material.

Data processing and kinematic model

All the joint angles were computed using principles of mechanics (Zatsiorsky 1998; Jazar 2010). The trial duration from ~3.6 to 4.25 seconds was considered as static posture (i.e. 70 samples) since the change in joint angles were not significant after 3.6 seconds across postures and last few samples were dropped for avoiding the end of the trial effect. Joint angle data was filtered using second-ordered zero-lag low pass Butterworth filter. Cut-off frequency for the filter was set to 4.5Hz for removing any possible effect of physiological tremors in static postures. The frequency content of these tremors have been reported to be in multiple ranges of frequencies (Deuschl et al 2001; Fahn et al 2011; McAuley et al 2000). The general agreement between these studies is that tremor frequencies are below 5 Hz, although maximum frequencies vary. Our goal was to compare static postures (not movements), hence we chose a low value of cutoff frequency. We constructed matrix of size 35,000 (5 trials x 100 postures x 70 samples per posture) x 21 (dimension) from the entire data for each subject. We used this matrix for further analysis.

The hand model has twenty-one degrees of freedom (DoF) as shown in Figure 1 (B) (similar to Rezzoug et al., 2008). In this model, each finger is considered to have four DoFs: it includes flexion-extension (Flex-Ext) of DIP and PIP joints; it also includes flexion-extension and abduction-adduction of MCP joint. Thumb is represented with five DoFs which includes flexion-extension of IP and MCP joint, and three DoFs flexion-extension, abduction-adduction and axial rotation from CMC joint.

Exploring kinematic synergy space using a linear method

There is a strong relationship between DIP and PIP joint angles for I, M, R and L. DIP Vs PIP joints across twelve subject shows there is a strong linear relationship (r^2=0.997) between these joints across fingers. Dependency and amount of co-dependency may vary. However, covariation patterns are stereotypical. For quantification of variance explained by PCs, we used Principal Component Analysis (PCA). Static hand postures were transformed from joint angle space to space with basis vectors orthogonal to each other (i.e. “synergy space”) using PCA method. The dataset (35000 samples= 5 trials x 100 postures x 70 samples per posture) were analysed.

Dimensionality of the dataset is 21 considering 21DoFs hand model. We performed PCA by centering the data and using Singular Value Decomposition (SVD) algorithm. Variance explained by principal components in synergy space are plotted across subjects.

Posture Similarity Index (PSI)

Comparing two different hand postures in the synergy space, rather than in joint angle space may provide insightful information about overlap (in terms of synergy components) between two postures. The measure developed by us compares two hand postures in synergy space and gives a quantification number which is called as posture similarity index (PSI).

Theoretical formulation

Joint angle space spanned by various hand movements is also termed as *action manifold* (Feix et al., 2013). Our objective is to find a subset of postures that may help in exploring 21-dimensional space in the best possible way. A set of extreme postures were also included in the study which may help in exploring individual degrees of freedom of hand. One approach to study hand postures in synergy subspace is dimensionality reduction (Santello et al 1998). An alternative view is that the control signal helps controlling multiple degrees of freedom simultaneously (Todorov, 2002; Todorov et al., 2004). In synergy space, some postures might be similar to others. Due to such similarity between postures, it is possible to derive one posture by slight modification in synergies of a slightly different posture. However, if two postures are very different, it is not expected that slight modification of synergy of one posture will lead to the other posture. Quantifying similarity between postures will help us find representative postures. For each subject, the dataset contains 100 static hand postures and 35000 (5 trials x 100 postures x 70 samples per posture) samples with 21 dimensions. Since there is no learning or history effect between trials of a posture, we selected a random trial from five trials for every posture separately, resulting in 100 selected trials per subject (one trial per posture). Essentially, we assume that any one of the five trials is representative of the 5 trials performed. Note that there

"average" of the five trials may not represent each individual trial. We used PCA to project static hand postures from joint angle space to synergy space. Column-wise normalization was performed for all joint angles before applying PCA.

Let original dimensions of the data space be D (in this case dimensionality is 21, refer Figure 1 (B)). Projection matrix (W, dimension NxN) is created using all static posture samples (35000) that will transform static posture from joint angle space to multidimensional synergy space. All static postures are projected along eigenvectors separately using projection matrix (W) giving projected values (70xN). Note that in our case, static posture has dimensions of 70x21 (70 data points and 21 joint angles).

The covariance matrices ($\Sigma(i)$, dimension NxN (i.e. 21x21); for i=1 to 100) were computed from projected postures in feature space for each posture (70xN) separately. Diagonal elements of Σ represent the amount of variance in each PC direction. Variances (σ^2) are expected to be similar for similar postures. The ratio of variances (*i.e.* $F=\sigma^2_{1,1}/\sigma^2_{1,2}$) for two similar postures will be closer to 1. If postures are not same, the weighted ratio (i.e. λF) will give two different values. To avoid mathematical ambiguity, we always chose F less than one in all cases.

Weights were assigned to F ratio based on eigenvalues (λ) of PCs. The summation is performed across all the N PCs for generating *posture similarity index (PSI)*. *PSI* is expected to be higher for two similar postures in synergy subspace.

$$F_n^{i,j} = \frac{\sigma_{ni}^2}{\sigma_{nj}^2} \quad (1)$$

Where F is ratio of two variances in the n^{th} PC direction.

$$PSI(i,j) = \sum_{n=1}^{N} \lambda_n F_n^{i,j} \quad (2)$$

Where i, j represents similarity between i^{th} and j^{th} posture. λ_n represent Eigen value of n^{th} Eigen vector. PSI is the weighted sum of all variance ratios across N dimensions.

221 **Evaluation of PSI on Synthetic data**

222 To test the performance of our approach, we decided to first test the algorithm on a synthetic data
223 set. Three synthetic postures were generated using multivariate normal distribution using
224 following mean values and standard deviations. For posture 1 (mean ± S.D in X, Y, and Z, 5 ±
225 1.85, 2 ± 1.78, 10 ± 2.42), for posture 2 (mean ± S.D in X, Y, and Z, 10.54 ± 1.85, 7.35 ± 1.78,
226 17.25 ± 2.42). Mean for 2nd posture is generated using following equation:

$$\boldsymbol{Mean\ (p2) = mean\ p1 + 3 * \sigma(p1)} \quad \textbf{(3)}$$

227

228 For posture 3, (mean ± S.D in X, Y, and Z, 5.69 ± 0.694, 2.611 ± 0.61, 11.021 ± 1.02) used for
229 generating data points. Mean for 3rd posture was near to 1st postures since we would like to
230 overlap the data. Mean for 3rd posture is calculated using below equation:

$$\boldsymbol{Mean\ (p3) = mean\ p1 + 1 * \sigma(p3)} \quad \textbf{(4)}$$

231

232 Synthetic postures, each containing 500 samples were generated. The variance of posture 1 and
233 posture 2 are same which is (3.42, 3.17, 5.83), the variance of posture 3 is smaller than other
234 postures (0.48, 0.37, 1.043). Mean of posture 1 (represented in red) and posture 3 (represented in
235 blue) are closer to each other and mean of posture 2 (represented in green) is far. Variance for
236 posture 1 and 2 are similar but posture 3 has smaller variance and orientation of posture 3 data is
237 different in the space. There is an overlap between posture 1 and 3 as shown in Figure 3 (A). We
238 deliberately chose such a data set to check if our method can capture the details described above.

239 (Figure 3)

240 Data was normalized before application of PCA. PCA is performed for extracting kinematic
241 synergies from simulated dataset. 1st principal component (synergy) explains approximately 77%
242 of the variance, 2nd principal component explains approximately 15% of the variance and 3rd
243 component explains approximately 6% of total variance. This is illustrated in Figure 3 (B).

244 We used projection matrix W (3x3) to project data (1500x3) on synergy space/global PC space.
245 Covariance matrices (Σ_i 3x3, for i=1:3) was computed for the projected dataset. Diagonal
246 elements of covariance matrix represent projection of each posture in PC direction.

The projection ratio in each PC direction is computed and presented in Supplemental Table S1.

Each ratio ($F_n^{i,j}$) is computed as given in equation (1) is multiplied with respective Eigenvalues (λs) and finally added. This exercise was performed for all the postures and posture similarity matrix was developed. Each element in the matrix represents *posture similarity index* comparing amount of similarity between two postures.

The ratio is selected based on the condition that we chose F to be less than unity. The magnitude of each Eigenvector is 0.062, 0.0127 and 0.0054, elements for *PSI* matrix is computed using equation (5):

$$PSI_{i,j} = \sum_{n=1}^{3} \lambda_n * F_n^{i,j} \quad \textbf{(5)}$$

From the matrix of posture similarity in Supplemental Table S2, we can observe that posture 1 and 2 are more similar in comparison with posture 1 and 3 and posture 2 and 3. Posture 1 and 2 has same variance and structure is similar with shifted mean. However, posture 1 overlaps with posture 3 which has closer mean value but the structure of posture 1 is different from posture 3. We note that this method (PSI) preserves the inherent structure of the data. PSI index is not only mere quantification of overlap of two postures 2D space, rather it compares the similarity between two postures in the multidimensional synergy space. The advantage of using synergy space is that the reproduction of joint angles is relatively accurate. A large value of PSI index between two posture shows that there is a greater overlap of two postures in synergy space. If the value of PSI is smaller between two postures shows that large changes in synergies are required in kinematic space.

In this example of synthetic data, the value of PSI is 0.0757 between posture 1 and 2, whereas PSI is 0.0587 between posture, 1 and 3. In this case posture 1 and 2 are more similar in comparison with posture 1 and 3. Structure and variance (S.D.) are different for posture 3 from posture 1 and 2. Hence we need more synergies for transforming from posture 1 to 3.

Normalization was performed for the PSI matrix using following equation (6), variant normalization.

$$Normalized\ PSI_{i,j} = \frac{PSI_{i,j}}{\max(PSI_j)} \quad (6)$$

Normalized PSI index gives the values for posture 1, 2 and 3 listed in Supplemental Table S3.

PSI for experimental test dataset

Posture similarity index (PSI) was obtained for real experimental data. Each posture contains seventy samples and 21-dimensional data. Single posture was randomly selected with three different trials for purpose of illustration. Data was normalized before transforming from joint angle space to synergy space using PCA. 1st synergy component explains nearly 63% of the variance. 2nd synergy component explains roughly 23% of total variance and 3rd synergy component explains around 9% of the variance. Scree plot is shown in Figure 4.

(Figure 4)

Kinematic synergies generated by PCA by projecting joint angles on synergy space will give 21 different synergy components.

We consider all the 21 PCs for further analysis. Projection matrix W (21x21) was used for transforming from joint angle space to synergy space. Covariance matrix (Σ_i for i=1:21, 21x21) was computed for individual postures in synergy space. Diagonal elements of covariance matrix explain variance in each PC direction. Individual PC ratio (F) is multiplied by respective weights (λ) and summed for generating PSI index are present in Supplemental Table S4.

Normalized PSI is presented in Supplemental Table S5.

Normalized PSI index shows that postures are highly similar to each other in synergy space. This is expected since we performed analysis for a single posture with different trials. Note, however, even for the same posture, across different trials, PSI is not expected to be the theoretical maximum of 1, since even though it may be the same posture functionally, the exact joint angles may vary and hence PSI may not reach the theoretical maximum. So, in this case, since we chose the same posture (but different trials), so that the data has a relatively large overlap..

This example shows that our method works well both on real experimental and synthetic data in synergy space. An advantage of this method is it compares and quantify similarity in synergy

space rather than joint angle space. Finding PSI for set of hand postures, will give quantification measure from the perspective of overlap in synergy space.

Representative postures

For finding representative postures, we further used PSI for identifying the most important, defining set of postures ("eigen postures"). Column-wise PSIs are added which represents overall similarity that a posture has with all other postures. All the PSI values are added row-wise gives total PSI value. Using these values, relative PSI index has been developed using following equation (7)

$$Relative\ PSI_c = \frac{\sum_{i=1}^{100} PSI_{c,i}}{\sum_{i,j=1}^{100} PSI_{i,j}} \quad (7)$$

Where C is column-wise PSI value. Further, we sorted the relative PSI in ascending order. The left most element represents the posture with lowest similarity and as we move from left to right relative PSI index increases. The right most element shows maximum relative PSI. Cumulative relative PSIs were computed by summing the sorted relative PSI curve. The first derivative of cumulative relative PSI was calculated and its peak was determined. Postures on the right-hand side of the peak value are representative posture. These postures are also called as *Eigen postures* which help in deriving other postures based on kinematic synergies. The representative postures are more associated with many of the postures from a synergy point of view.

It is not expected that different subjects will have the peak of the derivative of relative PSI at the same number of posture. Also, it is not necessary for the same postures to lie on the right side of this peak. In other words, it is not theoretically necessary for the same postures to be representative for all subjects. The most frequent postures found among representative postures in different subjects has been computed and presented in results.

Results

Kinematic synergy using linear method

(Figure 5)

As shown in Figure 5, DIP vs PIP joint angle shows that there is a strong linear relationship (r^2=0.997) between joint angles of DIP and PIP. These results are in line with the previous study (Cerveri et al., 2007; Cobos et al., 2008; Cobos et al., 2010; Bullock et al., 2012).

We performed PCA by centering data and using Singular Value Decomposition (SVD) algorithm. Results were averaged across subjects and presented in Figure 6. From the Figure 6, we observed that in synergy space 1st PC explains approximately 40% of total variance and nearly first 5 PCs explained 84% of total variance in data. First 10 PCs explain approximately 95% of the total variance.

(Figure 6)

Static joint angles were reconstructed using 1st N PCs (i.e. Synergies) where N varies from 2 to 21. As expected, joint angle reconstruction error reduces as more number of kinematic synergies are involved. Joint angle reconstruction error was computed across all joints, across twelve subjects as shown in Figure 7. The shaded region represents standard error of mean across subjects.

(Figure 7)

From the result in Figure 7, we find that the error in joint angle reconstruction is higher while considering few synergy components, one of the possible reasons is task involved in the experiment. The experiment does not involve only activities of daily living but also includes ASL and aesthetic (Bharatanatyam) postures.

The *posture similarity index* analysis was run for all subjects separately. For analysis, one out of five trials were selected randomly for all 100 postures. PSI matrix (100x100) gives the similarity between any two postures in the dataset. PSI matrix for a single subject is shown in the Figure 8.

(Figure 8)

Based on the PSI matrix is shown in the Figure 8, posture 11 was selected and compared with rest of the postures for illustration purpose. In the Figure 9, postures are presented in the descending order of posture similarity index for top five PSI values.

(Figure 9)

Based on PSI value, posture 11 is most similar to posture 15, other postures such as posture 37, posture 58, and posture 3 shows similarity in descending order respectively. Posture 11 and 15 shares common features such as the posture of the thumb. However, posture of other fingers is different. The high similarity between posture 11 and 15 means that there is greater overlap between these postures. Posture 37 also shares similar thumb position as posture 11 gives large PSI value. In posture 58, Index and middle fingers are straight similar to posture 11 which cause larger similarity but ring and little fingers are flexed. Posture 3 shares common features such as the abduction of middle, ring and little finger which results in high PSI value. For each subject, PSI matrix was unique.

Representative postures

For finding representative postures, relative PSI values were computed by summing all the PSI values for a posture and find ratio with total PSI value of a matrix for each posture separately as shown in Figure 10 (A). Postures were rearranged based on relative PSI index in ascending order and taken first derivative of relative PSI as shown in Figure 10 (B).

(Figure 10)

The peak value for all each subject was measured. For comparison, we used smallest peak across subjects as the peak. Since the representative postures are not expected to be same across subjects, we present the most frequent postures in Table 1 (only those postures found in 7 subjects are more are presented here for illustration purpose and brevity).

(Table 1)

Statistical analysis

Many representative postures in the dataset includes more special postures rather than common postures. However, the number of special postures used in the experiment were comparatively more than common postures. To rule out the possibility that the representative postures have more special postures purely because they were larger in number in the overall dataset, we normalized the number of representative postures by the respective number of postures present in the actual dataset separately for special and common postures. Paired t-test shows that the

number of common postures is significantly lesser than the number of special postures in a set of representative postures. Further, we performed one-way repeated measures ANOVA, with the type of posture (i.e. common Vs special) as a factor on the number of postures present in the representative postures. We found that the number of special postures is significantly higher than the number of common postures (Mean ± error, common Vs special: 16.91 ± 0.96 Vs 29.75 ± 0.98). These findings revealed that for the given dataset more number of special postures are represented in in synergy subspace in comparison with common postures. This result is illustrated in Figure 11 below.

(Figure 11)

Discussion

This article showcases a novel approach for comparing hand postures using synergies (PCA). Our method exploits use a ratio of variances in eigen directions generated by PCA for comparison of two static hand postures. Posture similarity index (PSI) is a measure of similarity of two postures in the synergy space. We used idea further for identifying representative postures from the large pool of various postures including common postures (activities of daily living; ADL) and special postures. Our approach which involved combining the inherent structure of hand postures allows the relative comparison of the overlap in synergy space between two postures. We use this to further identify a set of representative postures. We discuss the implications of our findings.

Kinematic synergies during performance of a dynamic task:

In the literature, several studies have documented evidence for synergies in constrained and unconstrained exploration tasks. These have involved environmental constraint exploration, unconstrained exploration and grasping of real and imaginary objects etc., (Santello et al 1998). Thakur et al., (2008) documented the existence of task-independent synergy components across several tasks, while the subjects were blindfolded and were allowed relatively free haptic exploration of several real-life objects. They also found that some of these synergies are similar across several subjects. In more recent studies, (Della Santina et al., 2017, Eppner et al., 2015) constrained exploration has been used to document the existence of kinematic synergies. In our

study, we have used one hundred different postures, comprising relatively new ("special postures", including ASL, Bharatanatyam postures) and familiar ("common", daily life postures) in addition to some real-life object grasping postures. Our results from synergy perspective are in-line with previous studies (Santello et al 1998). However, it must be noted that in our study we have analysed static posture (70 data samples per trial per posture), but not the actual movement (kinematics involving exploration, pre-shaping). Our goal here was to develop an index that captures similarity of postures in the synergy space. Hence, we considered each posture and compared with the other postures within the synergy (PCA) space. Hence, our "representative postures" are representative among the 100 postures considered, but not a combination of several postures as in synergies. Since we used a relatively large number of postures, we believe that our representative postures could be representative in the real-life sense, although this is just speculation, since the human hand can perform a myriad number of tasks and our postures considered are only 100 of those.

Use of human hand synergies in development of robotic hands:

A crucial application of human hand synergies involves the development of dexterous robots and prosthetic devices. Synergy based robotic hands have been documented by several groups (Ciocarlie & Allen 2009, Brown & Asada 2007, Fani et al., 2016). It is unclear, however, if anthropomorphism is the best possible strategy for using synergies in building better robotic hands (Santello et al. 2016). However, it can be argued in cases involving interaction of a human with robots, anthropomorphism is a desirable feature. It has also been suggested that a mechanism similar to motor synergies in hand may underlie the function of mirror neurons (D'Ausilio et al 2015). Anthropomorphism index (AI) has been used for comparing human hand posture with artificial hand using a projection of multi-dimensional posture into two-dimensional nonlinear subspace (Feix et al., 2013). The method uses a comparison of a cell to cell basis in two-dimensional space. However, this method assumes that we can reconstruct actual posture from two-dimensional nonlinear subspace. In our study, we develop the PSI, which compares two postures performed by humans in the synergy space. Here we project the postures to the synergy space to perform the comparison. PSI takes into account of the variance in all directions which assure accurate hand posture reconstruction. The large value of PSI represents high similarity between two postures that gives an indication of larger overlap of between postures.

Sometime PSI does not result in intuitive numbers while comparing two postures, possible major reason behind this because of degrees of freedom and the large number of tasks involved.

Representative postures and Synergies – Possible neural mechanisms:

Synergies are neuronal structural units which central nervous system uses as the basis for generating any new posture (Santello et al., 1998; Mason et al., 2001; Leo et al., 2016). In our study, we use representative postures, which are not elements of synergy, but rather individual elements that are most represented through multiple postural synergies. Several studies have documented evidence for synergistic movement of fingers through neural stimulating (Gentner and Classen, 2006; Gentner et al., 2010) in primary motor cortex similar to a study that involves grasping of imagined object (Santello et al., 1998; Leo et al., 2016). These findings provide strong support to the notion of the synergistic representation in brain areas. These postures represent large similarity in joint angle space. We believe our representative postures seek equal action manifold comparison to our large set of postures. Our finding also suggests that significantly large number of special postures are part of representative posture rather than common postures. We believe that this may be because overlearned tasks may be captured with a smaller number of synergies but the great behavioural flexibility in the human system may not be captured with a small number of synergies (Gentner et al., 2010). Hence, common postures occupy lesser space and more concentrated whereas special postures are spread across synergy space. Our method captures this effect reasonably well.

Concluding comments:

In this study, we have defined, developed and demonstrated the use of a synergy based posture comparison index, PSI. It is also useful to classify postures as “representative” or otherwise. A limitation of the current approach is that comparison between two hand postures depends on the complexity of hand model. Our hand model consists of 21 DoF model, which does not account for the palm arch and wrist joints. PSI may give more insightful results for a complex model involving multiple degrees of freedom. Distribution of data may provide more hidden information about hand postures and will be able to produce more accurate results.

References:

1. Brown CY., Asada HH. 2007. Inter-finger coordination and postural synergies in robot hands via mechanical implementation of principal components analysis. In: *Intelligent Robots and Systems, 2007. IROS 2007. IEEE/RSJ International Conference on*. IEEE, 2877–2882.
2. Bullock IM., Borràs J., Dollar AM. 2012. Assessing assumptions in kinematic hand models: a review. In: *Biomedical Robotics and Biomechatronics (BioRob), 2012 4th IEEE RAS & EMBS International Conference on*. IEEE, 139–146.
3. Cavallo A., Koul A., Ansuini C., Capozzi F., Becchio C. 2016. Decoding intentions from movement kinematics. *Scientific Reports* 6:37036.
4. Cerveri P., De Momi E., Lopomo N., Baud-Bovy G., Barros RML., Ferrigno G. 2007. Finger kinematic modeling and real-time hand motion estimation. *Annals of biomedical engineering* 35:1989–2002.
5. Ciocarlie MT., Allen PK. 2009. Hand posture subspaces for dexterous robotic grasping. *The International Journal of Robotics Research* 28:851–867.
6. Cobos S., Ferre M., Ángel Sánchez-Urán M., Ortego J., Aracil R. 2010. Human hand descriptions and gesture recognition for object manipulation. *Computer methods in biomechanics and biomedical engineering* 13:305–317.
7. Cobos S., Ferre M., Uran MS., Ortego J., Pena C. 2008. Efficient human hand kinematics for manipulation tasks. In: *Intelligent Robots and Systems, 2008. IROS 2008. IEEE/RSJ International Conference on*. IEEE, 2246–2251.
8. D'Ausilio A., Bartoli E., Maffongelli L. 2015. Grasping synergies: a motor-control approach to the mirror neuron mechanism. *Physics of life reviews* 12:91–103.
9. Della Santina C., Bianchi M., Averta G., Ciotti S., Arapi V., Fani S., Battaglia E., Catalano MG., Santello M., Bicchi A. 2017. Postural Hand Synergies during Environmental Constraint Exploitation. Frontiers in Neurorobotics 11. DOI: 10.3389/fnbot.2017.00041

10. Deuschl G., Raethjen J., Lindemann M., Krack P. 2001. The pathophysiology of tremor. *Muscle & nerve* 24:716–735.
11. Eppner C., Deimel R., Álvarez-Ruiz J., Maertens M., Brock O. 2015. Exploitation of environmental constraints in human and robotic grasping. The International Journal of Robotics Research 34:1021–1038.
12. Fahn S., Jankovic J., Hallett M. 2011. *Principles and Practice of Movement Disorders E-Book*. Elsevier Health Sciences.
13. Fani S., Bianchi M., Jain S., Pimenta Neto JS., Boege S., Grioli G., Bicchi A., Santello M. 2016. Assessment of myoelectric controller performance and kinematic behavior of a novel soft synergy-inspired robotic hand for prosthetic applications. *Frontiers in neurorobotics* 10:11.
14. Feix T., Romero J., Ek CH., Schmiedmayer H-B., Kragic D. 2013. A metric for comparing the anthropomorphic motion capability of artificial hands. *IEEE transactions on robotics* 29:82–93.
15. Gentner R., Classen J. 2006. Modular organization of finger movements by the human central nervous system. *Neuron* 52:731–742.
16. Gentner R., Gorges S., Weise D., aufm Kampe K., Buttmann M., Classen J. 2010. Encoding of motor skill in the corticomuscular system of musicians. *Current Biology* 20:1869–1874.
17. Hoyet L., Ryall K., McDonnell R., O'Sullivan C. 2012. Sleight of hand: perception of finger motion from reduced marker sets. In: *Proceedings of the ACM SIGGRAPH Symposium on Interactive 3D Graphics and Games*. ACM, 79–86.
18. Jazar, R. N. (2010). Theory of applied robotics: kinematics, dynamics, and control. Springer Science & Business Media.
19. Jerde TE., Soechting JF., Flanders M. 2003a. Biological constraints simplify the recognition of hand shapes. *IEEE transactions on biomedical engineering* 50:265–269.
20. Leo A., Handjaras G., Bianchi M., Marino H., Gabiccini M., Guidi A., Scilingo EP., Pietrini P., Bicchi A., Santello M., Ricciardi E. 2016. A synergy-based hand control is encoded in human motor cortical areas. *eLife* 5:e13420. DOI: 10.7554/eLife.13420.

21. Mason CR., Gomez JE., Ebner TJ. 2001. Hand synergies during reach-to-grasp. *Journal of Neurophysiology* 86:2896–2910.
22. McAuley JH., Marsden CD. 2000. Physiological and pathological tremors and rhythmic central motor control. *Brain* 123:1545–1567.
23. Rezzoug, N., and Gorce, P. (2008). Prediction of fingers posture using artificial neural networks. Journal of Biomechanics, 41(12), 2743–2749.
24. Roweis ST., Saul LK. 2000. Nonlinear dimensionality reduction by locally linear embedding. *science* 290:2323–2326.
25. Santello M., Bianchi M., Gabiccini M., Ricciardi E., Salvietti G., Prattichizzo D., Ernst M., Moscatelli A., Jörntell H., Kappers AM. 2016. Hand synergies: integration of robotics and neuroscience for understanding the control of biological and artificial hands. *Physics of life reviews* 17:1–23.
26. Santello M., Flanders M., Soechting JF. 1998. Postural hand synergies for tool use. *Journal of Neuroscience* 18:10105–10115.
27. Thakur PH., Bastian AJ., Hsiao SS. 2008. Multidigit Movement Synergies of the Human Hand in an Unconstrained Haptic Exploration Task. Journal of Neuroscience 28:1271–1281.
28. Todorov E., Ghahramani Z. 2004. Analysis of the synergies underlying complex hand manipulation. In: *Engineering in Medicine and Biology Society, 2004. IEMBS'04. 26th Annual International Conference of the IEEE*. IEEE, 4637–4640.
29. Todorov E., Jordan MI. 2002. Optimal feedback control as a theory of motor coordination. *Nature neuroscience* 5:1226.
30. Wheatland N., Jörg S., Zordan V. 2013. Automatic hand-over animation using principle component analysis. In: *Proceedings of Motion on Games*. ACM, 197–202.
31. Wu G., van der Helm FCT., Veeger HEJD., Makhsous M., Van Roy P., Anglin C., Nagels J., Karduna AR., McQuade K., Wang X., Werner FW., Buchholz B., International Society of Biomechanics 2005. ISB recommendation on definitions of joint coordinate systems of various

joints for the reporting of human joint motion--Part II: shoulder, elbow, wrist and hand. *Journal of Biomechanics* 38:981–992.

32. Zatsiorsky, V. M. (1998). Kinematics of human motion, Human Kinetics. Urbana Champaign.

Figure 1

Figure 1: (a) Sensor placement location on hand. (b) Kinematic hand model consisting of 21 DoFs.

(a) Fifteen sensors are placed on digits and one reference sensor is placed near wrist. (b) DIP and PIP joints corresponds to 1 DOF; MCP joint corresponds to 2 DOFs; for thumb CMC joint corresponds to 3 DOFs.

PeerJ Preprints | https://doi.org/10.7287/peerj.preprints.3080v2 | CC BY 4.0 Open Access | rec: 1 Jul 2018, publ: 1 Jul 2018

A

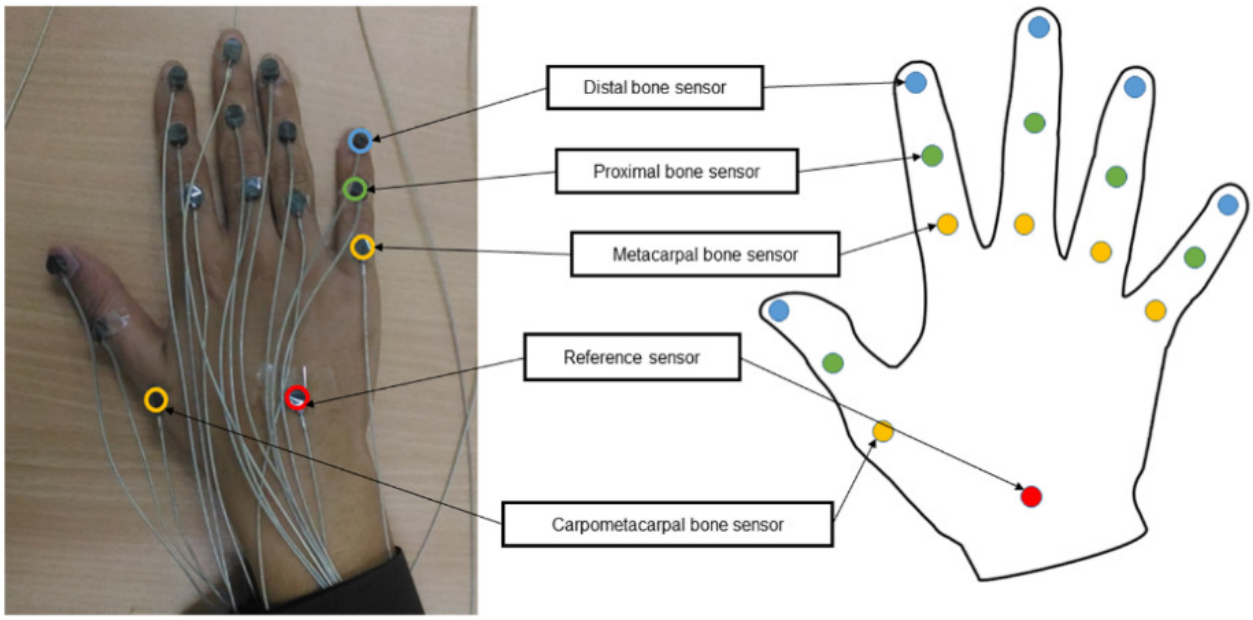
Distal bone sensor
Proximal bone sensor
Metacarpal bone sensor
Reference sensor
Carpometacarpal bone sensor

B

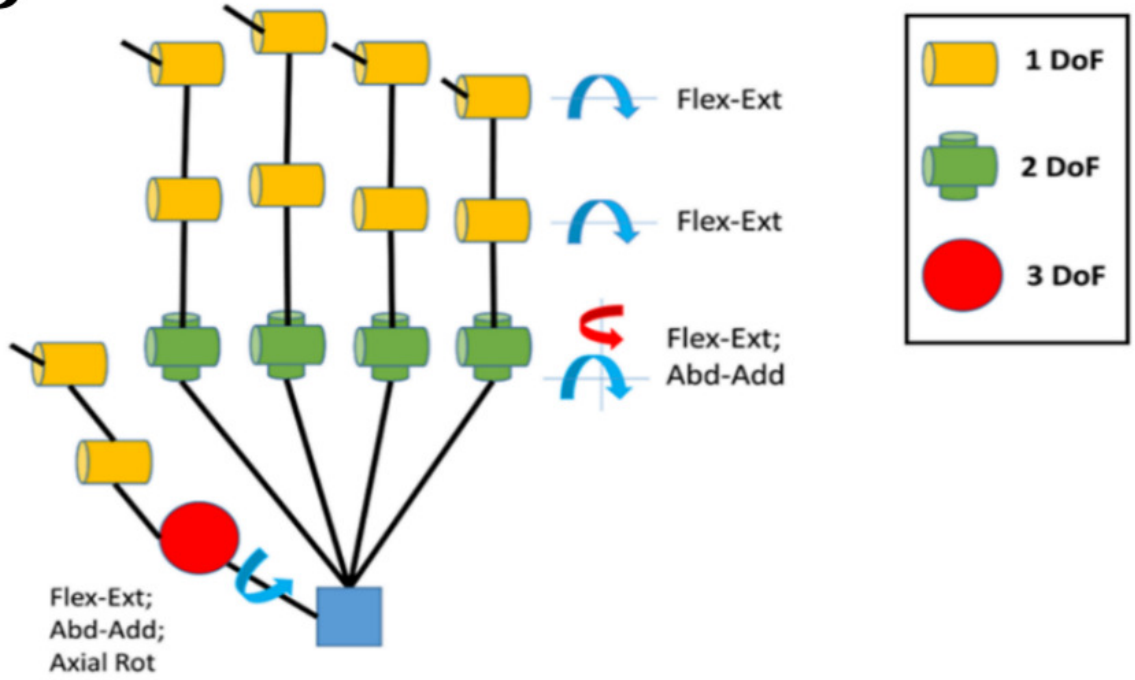
Flex-Ext
Flex-Ext
Flex-Ext;
Abd-Add
Flex-Ext;
Abd-Add;
Axial Rot
1 DoF
2 DoF
3 DoF

Figure 2

Experimental setup.

Subjects were seated in a height-adjustable chair. Placement of transmitter was based on biomechanical standards (Wu et al., 2005). The computer screen was placed approximately 1 m away from the subject. Image of posture was shown to the subject on the screen. Subjects were asked to perform posture which is shown on the screen starting from the base posture.

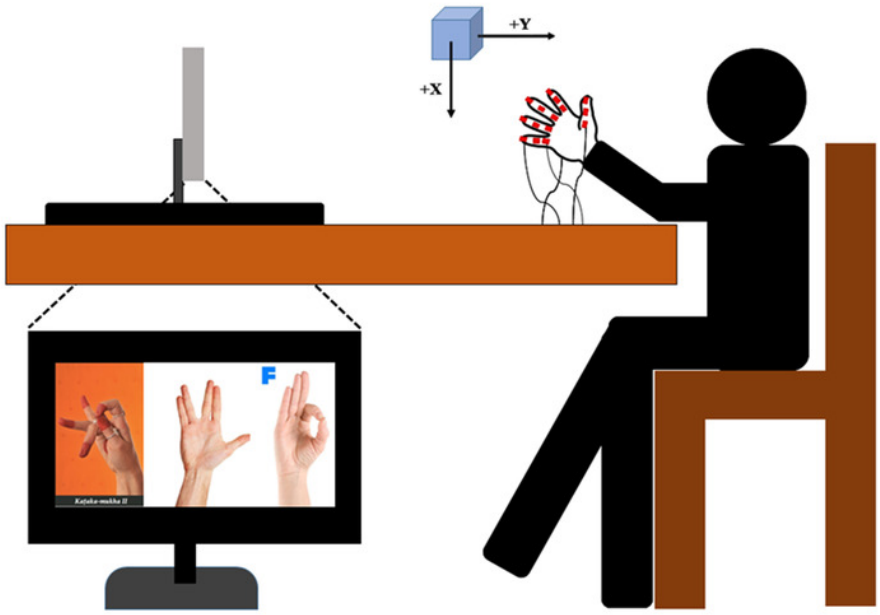

Figure 3

(a) Simulated postures in 3D space. (b) Variance in the synergy space for synthetic dataset.

(a) Posture 1 and posture 2 have same covariance matrix but different mean values. Mean of posture 3 is closer to posture 1, which means there is an overlap between posture 1 and 3. Structure of posture 1 and 3 are different. (b) Synergy 1 represents highest variance (i.e. ~77.8%), Synergy 2 explains (~15.8%) variance, and Synergy 3 explains (~6.7%) variance.

PeerJ Preprints | https://doi.org/10.7287/peerj.preprints.3080v2 | CC BY 4.0 Open Access | rec: 1 Jul 2018, publ: 1 Jul 2018

A

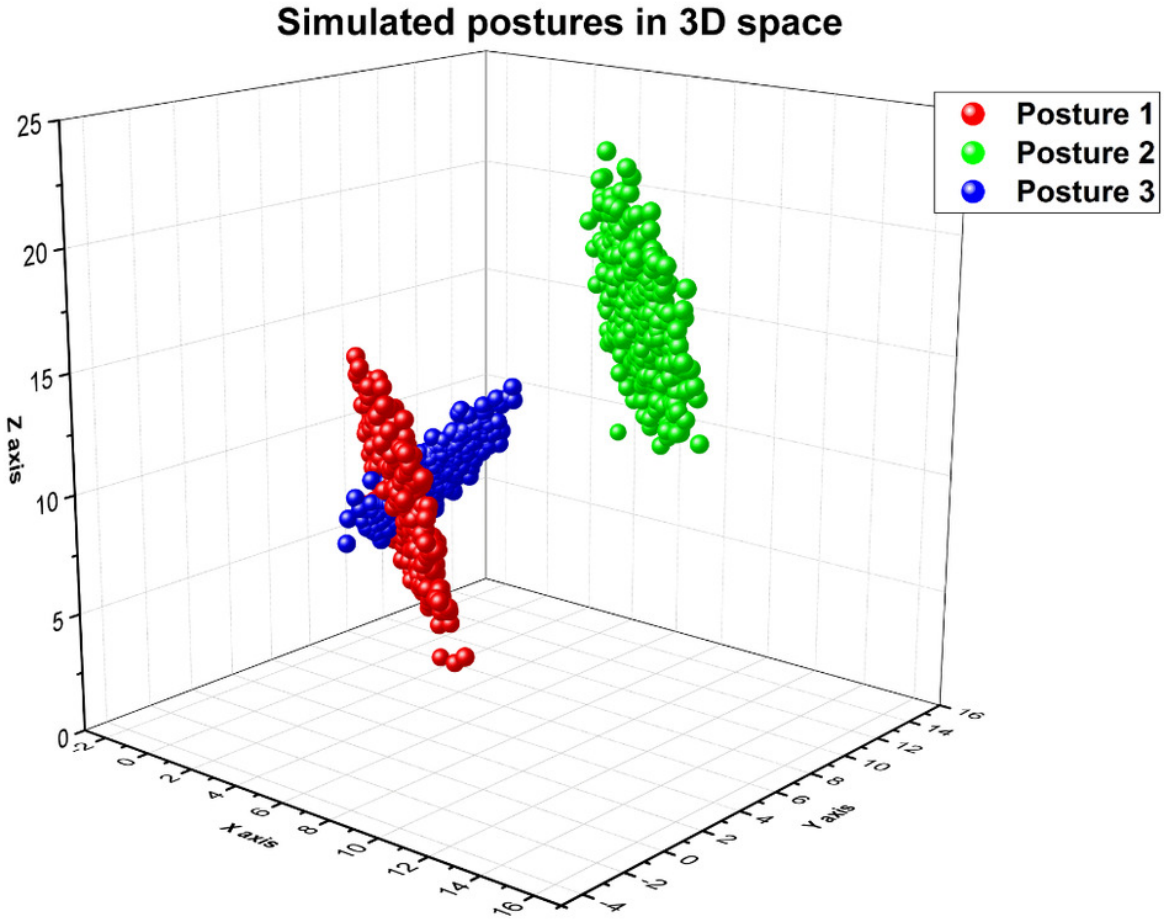
Simulated postures in 3D space
Posture 1
Posture 2
Posture 3
z axis
x axis
y axis

B

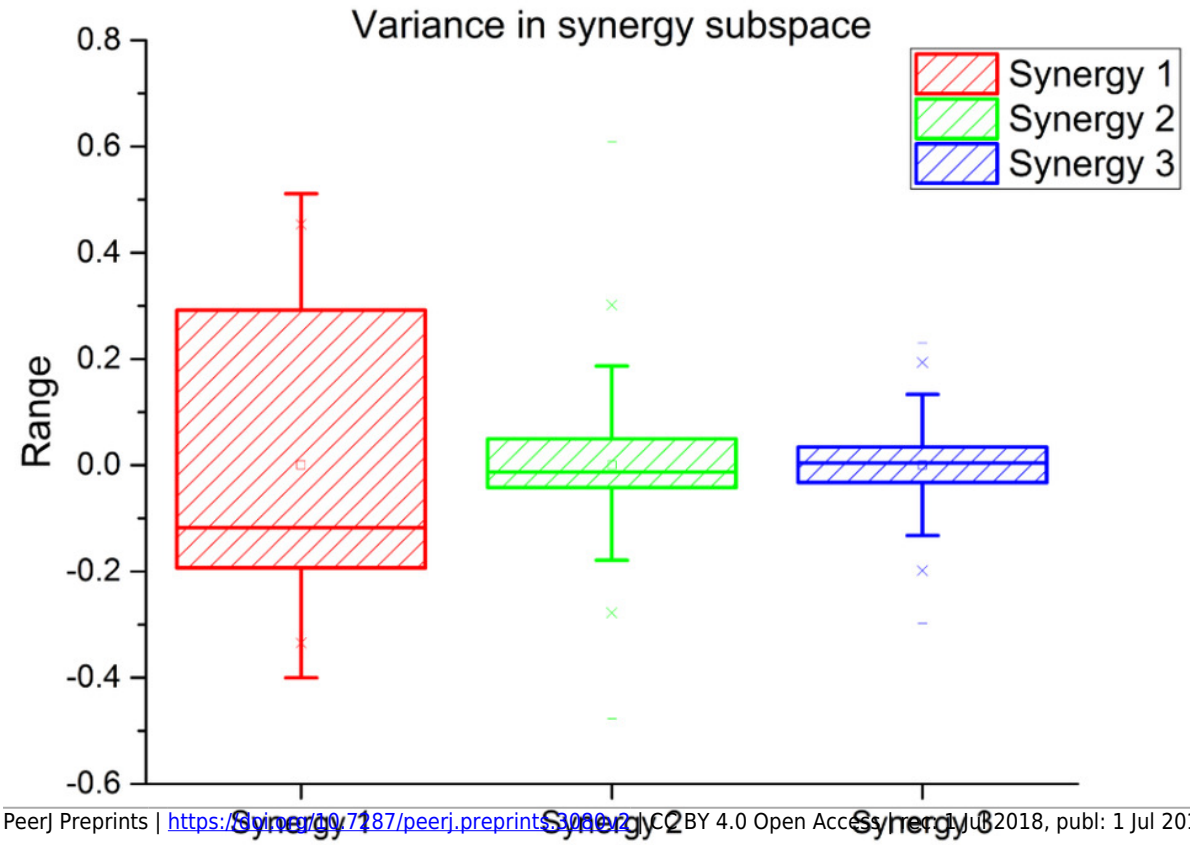
Variance in synergy subspace
Synergy 1
Synergy 2
Synergy 3
Range
Synergy 1
Synergy 2
Synergy 3

Figure 4

Scree plot for actual postures with three trials

PC1 explains approximately 63.6% of variance, PC2 and PC3 explains nearly 23% and 9% of variance respectively.

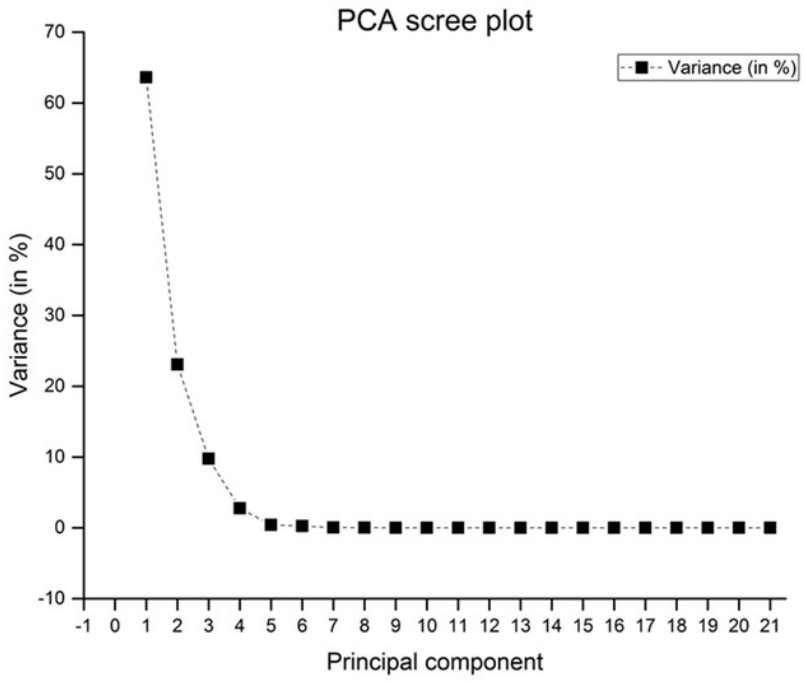

Figure 5

Mean value between DIP-PIP joints for a single trial across subjects

Joint angle relation between distal interphalangeal (DIP) and Proximal interphalangeal (PIP) joints.

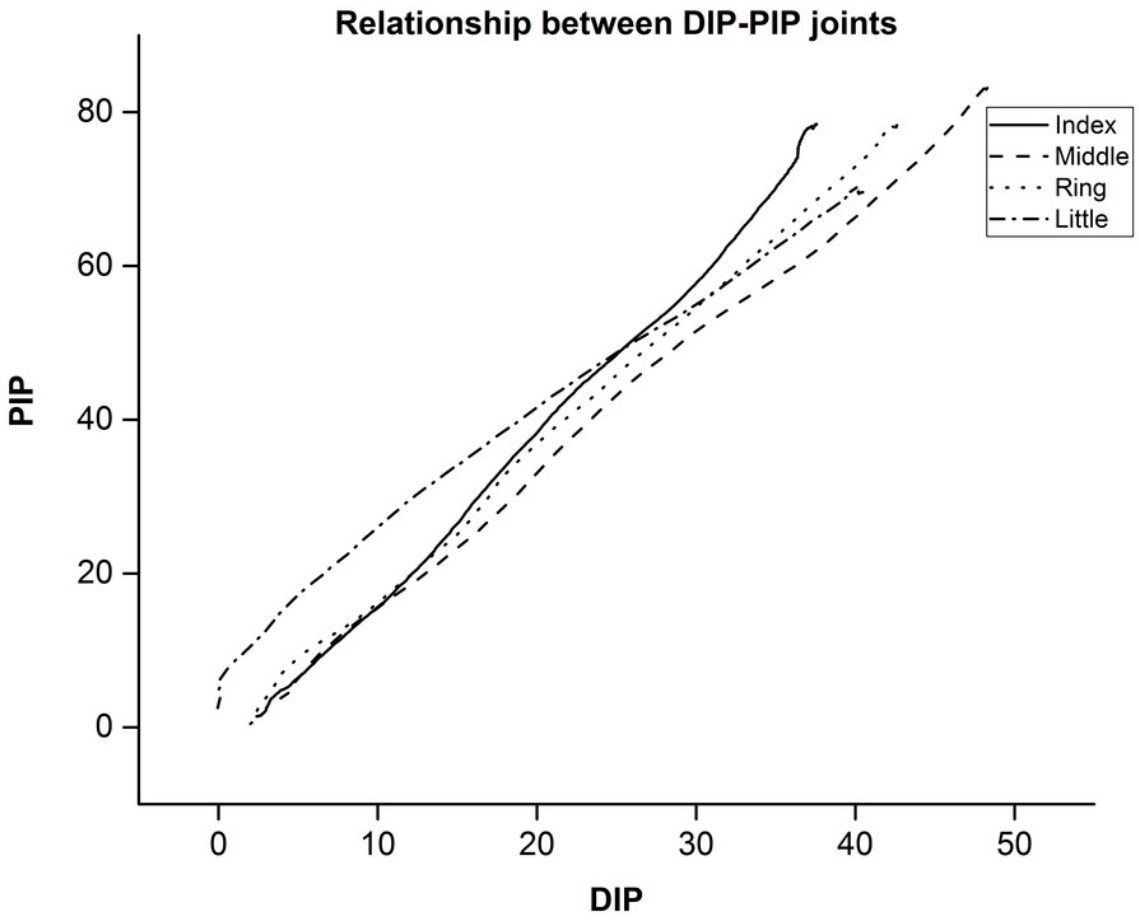

Figure 6

PCA variance explained by a principal component

1st PC explains nearly 40% of variance and 2nd PC explains nearly 20% of variance, error bar represents standard error of mean across subjects.

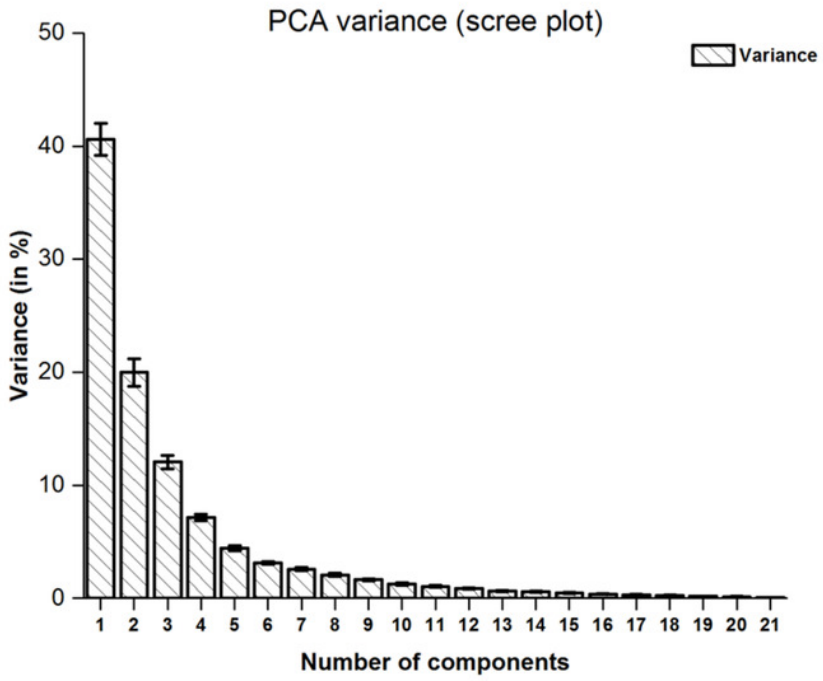

Figure 7

Joint angle reconstruction error.

Mean squared error across postures were plotted against number of synergy components counted. Joint angle reconstruction error reduces as more number of synergy components were introduced.

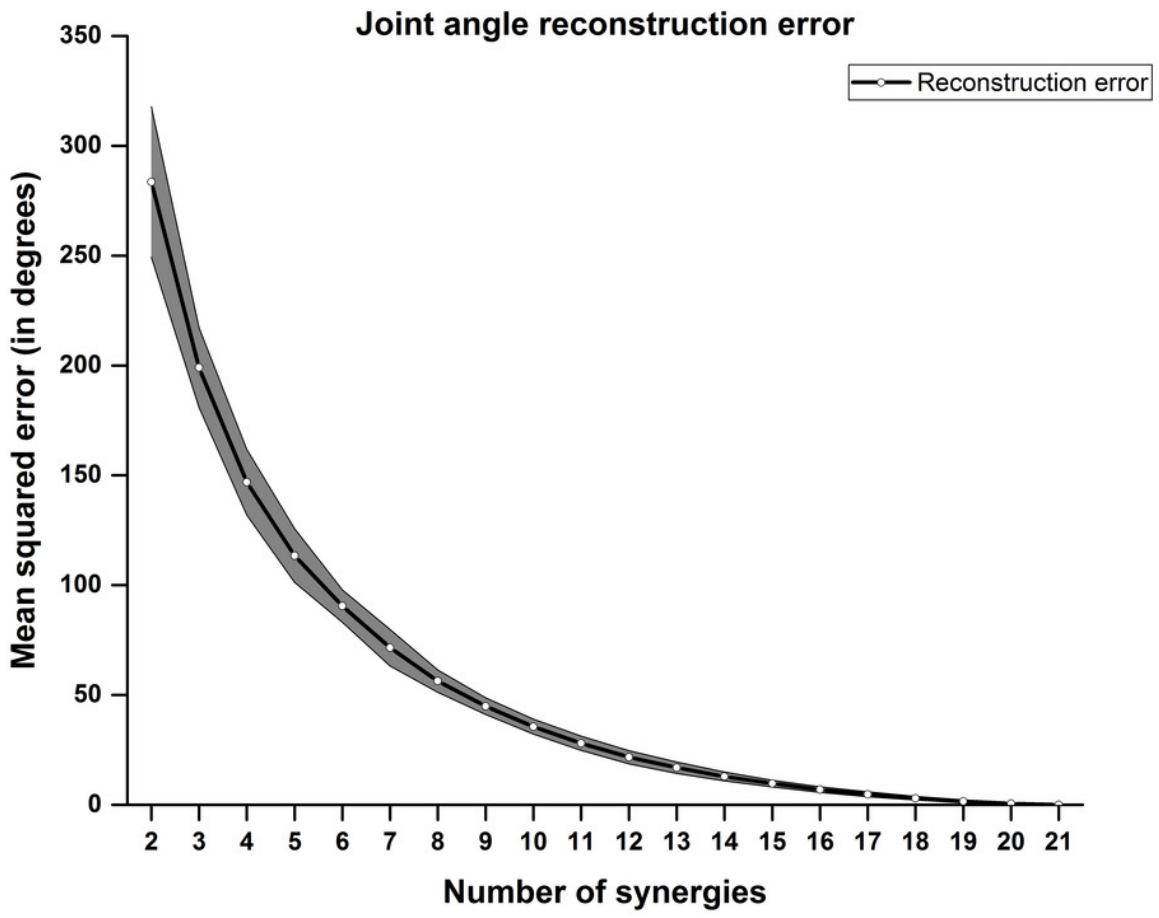

Figure 8

Colour map representation of PSI matrix.

Dark red colour represents very high similarity between postures in synergy space where as blue colour represents low similarity between postures.

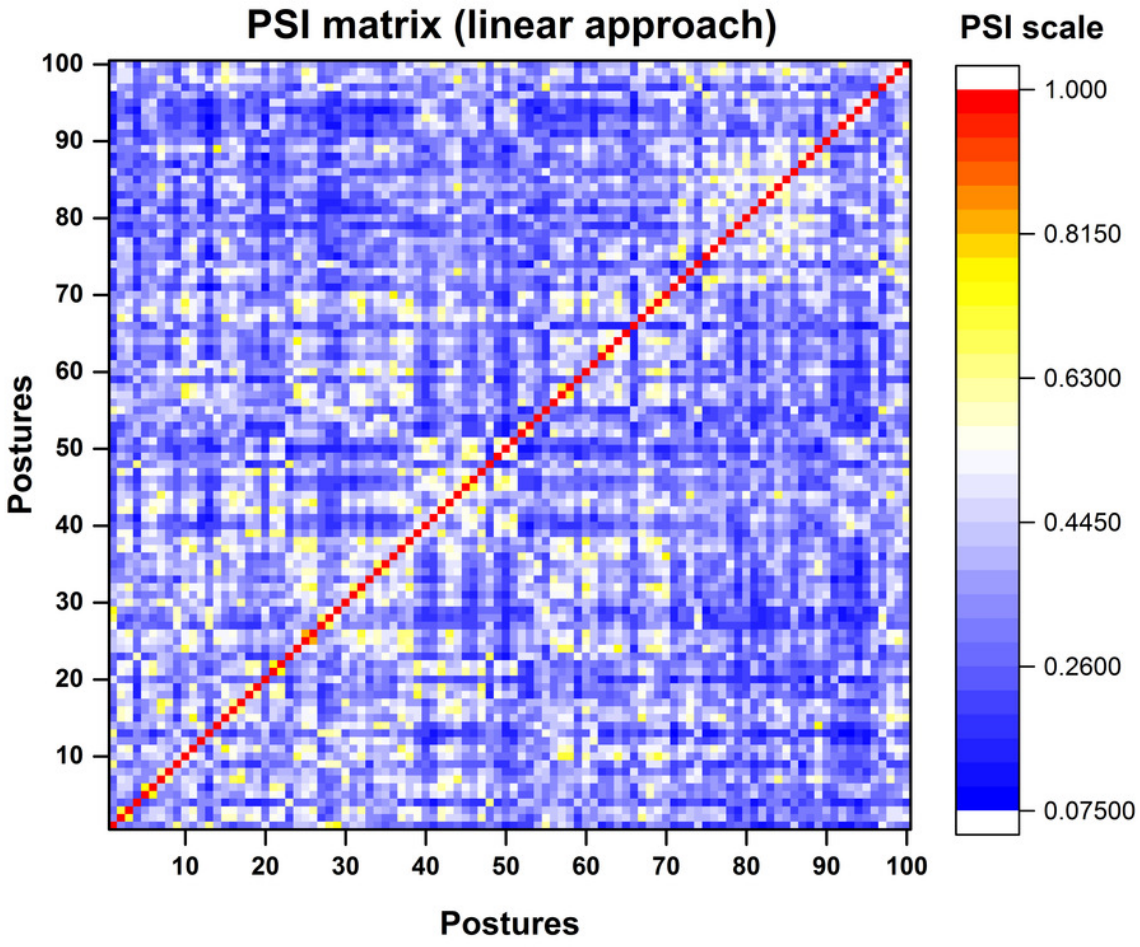

Figure 9

Top five Postures based on PSI values

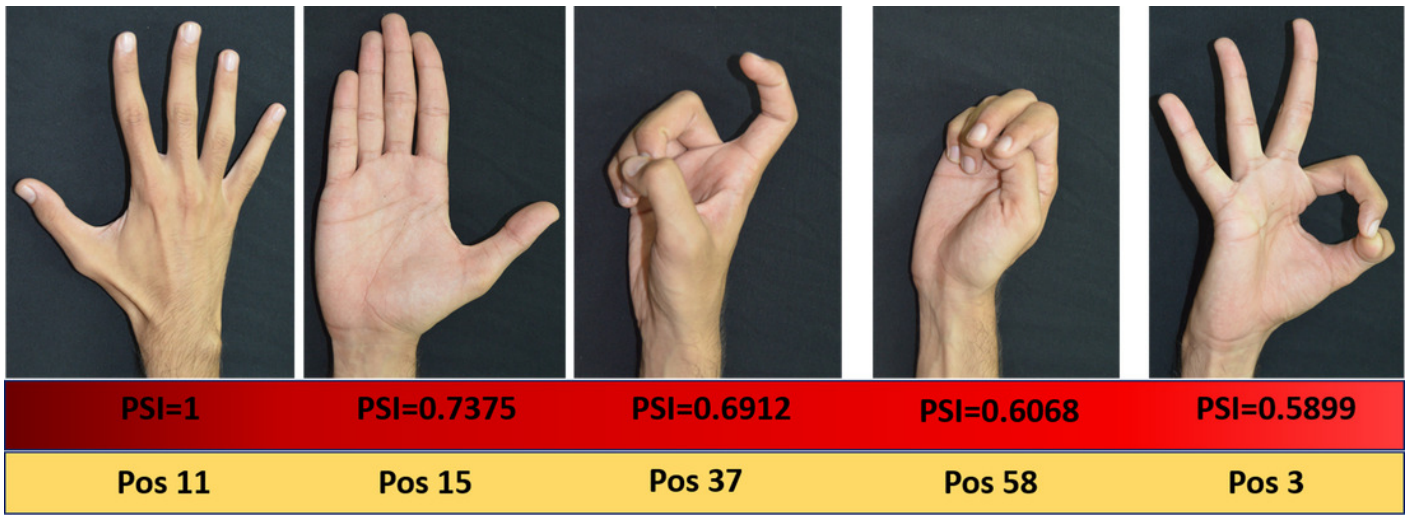

Figure 10

(a) Cumulative relative PSI index. (b) First derivative of relative PSI index for all subjects.

PeerJ Preprints | https://doi.org/10.7287/peerj.preprints.3080v2 | CC BY 4.0 Open Access | rec: 1 Jul 2018, publ: 1 Jul 2018

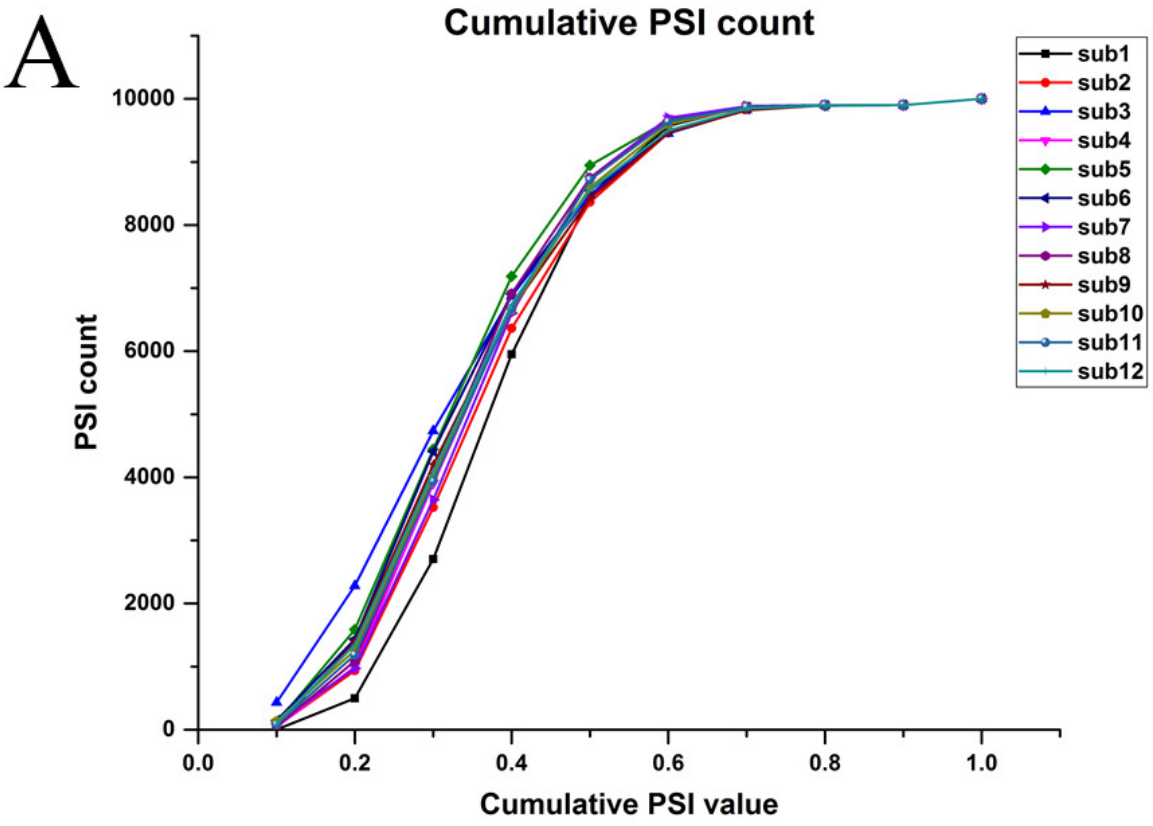
A
Cumulative PSI count
PSI count
Cumulative PSI value
0
2000
4000
6000
8000
10000
0.0
0.2
0.4
0.6
0.8
1.0
sub1
sub2
sub3
sub4
sub5
sub6
sub7
sub8
sub9
sub10
sub11
sub12

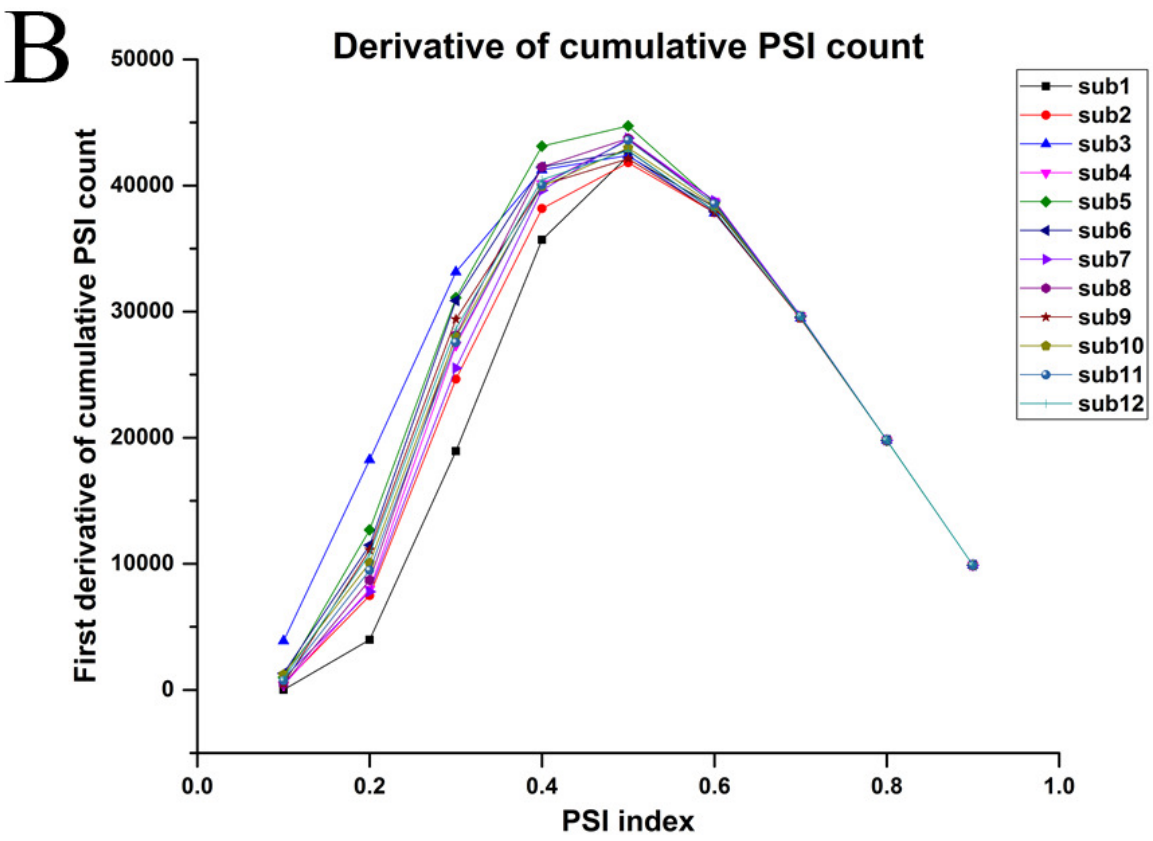
B
Derivative of cumulative PSI count
First derivative of cumulative PSI count
PSI index
0
10000
20000
30000
40000
50000
0.0
0.2
0.4
0.6
0.8
1.0
sub1
sub2
sub3
sub4
sub5
sub6
sub7
sub8
sub9
sub10
sub11
sub12

Figure 11

Task dependent representative posture count.

Number of representative special postures are significantly large in synergy space in comparison with common postures.

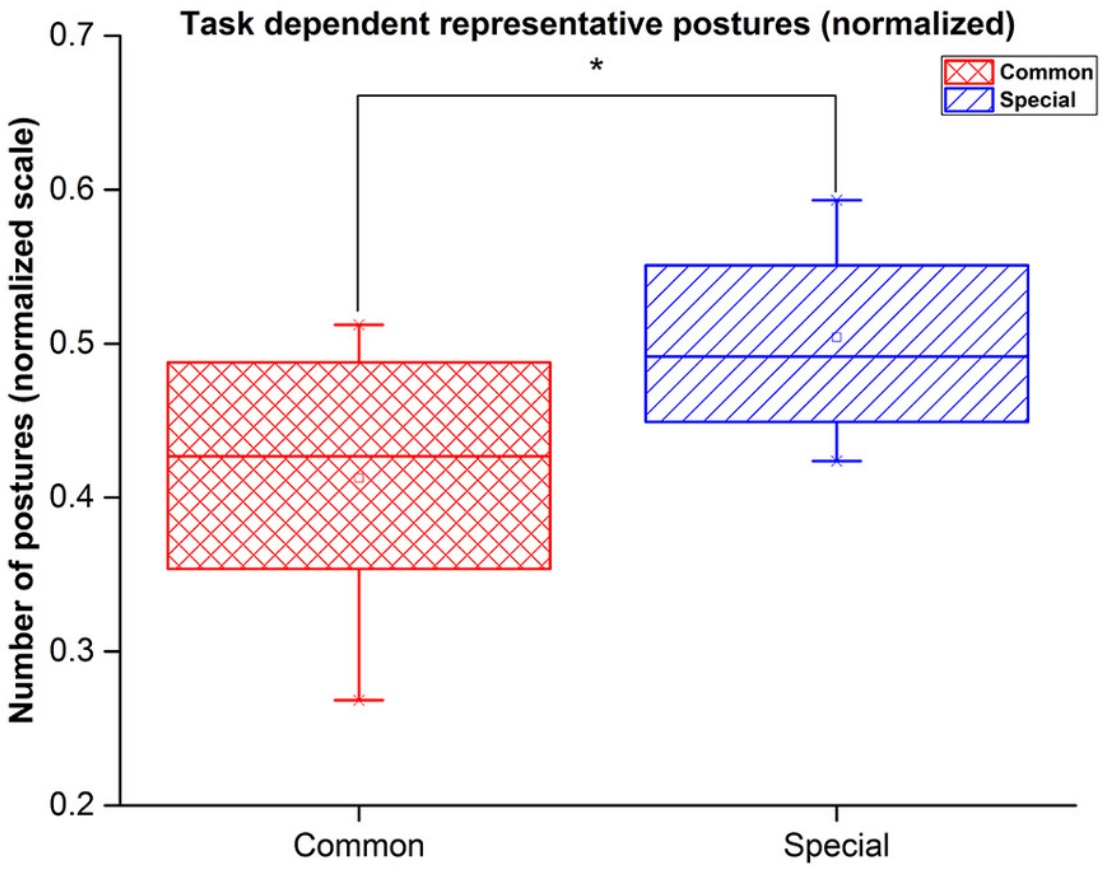

Table 1(on next page)

Table 1: Representative postures

Representative postures identified by PSI

1

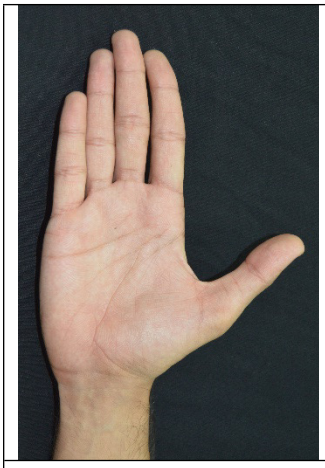

Most common representative posture- present in all 12 subjects

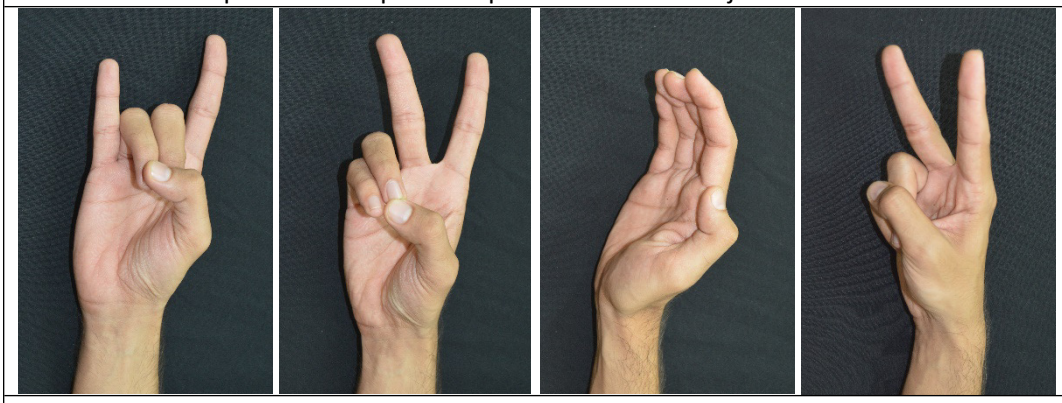

Present in 11 subjects

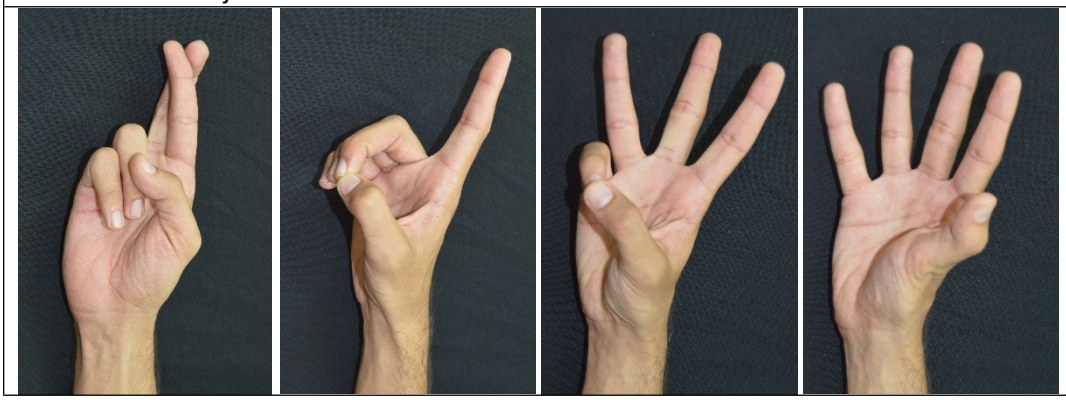

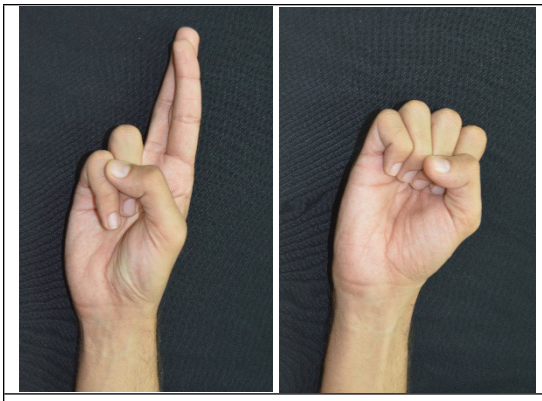

Present in 10 subjects

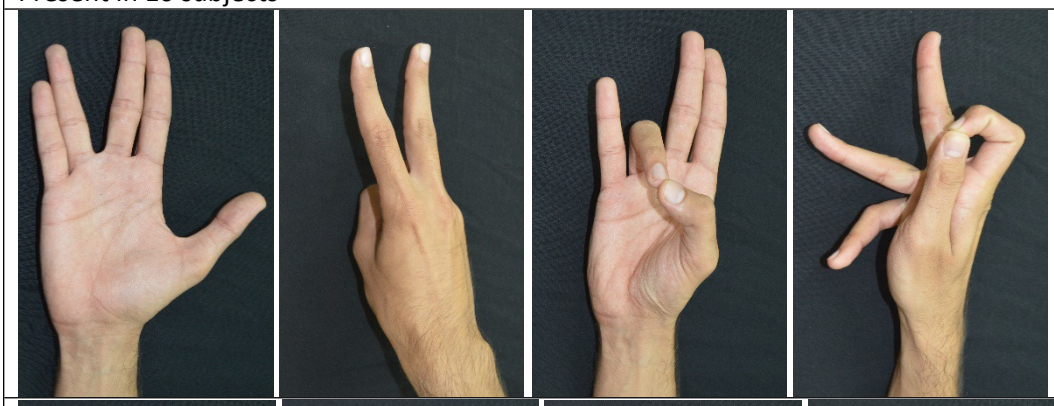

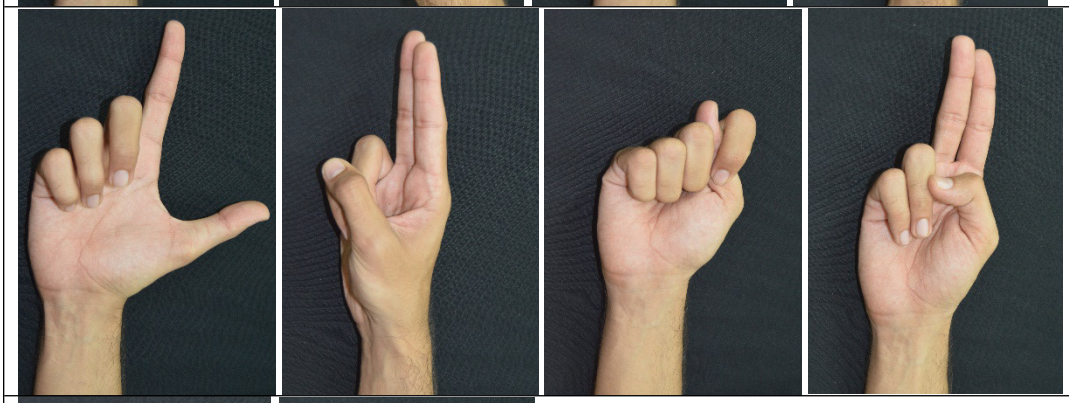

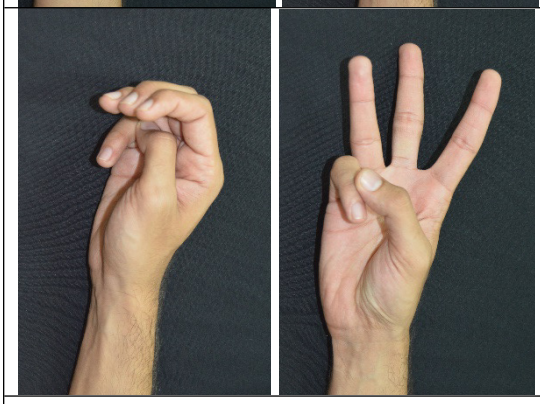

Present in 9 subjects

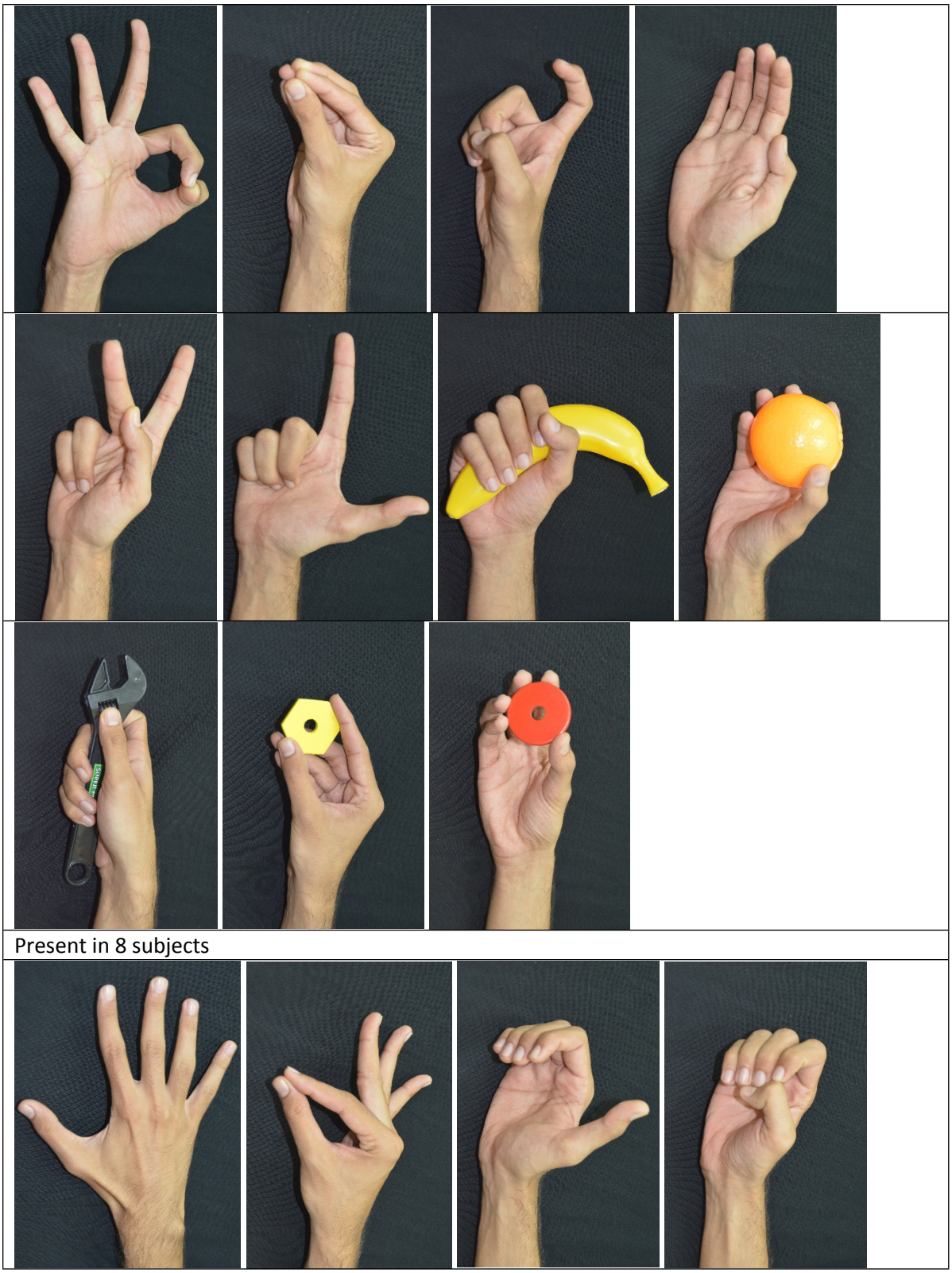

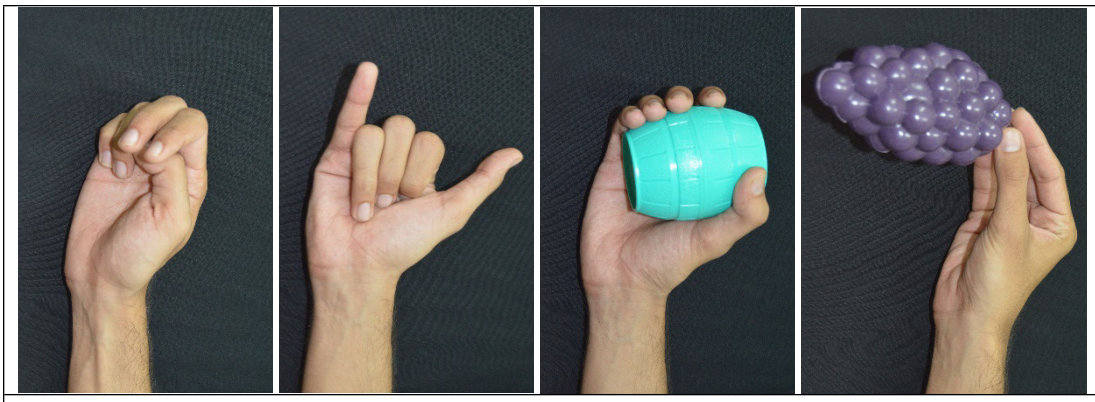

Present in 7 subjects